Reinforced Concrete Shell Elements Subjected to Bending and Membrane Loads

by Maria Anna Polak and Frank J. Vecchio

Large-scale reinforced concrete shell elements were tested under conditions of biaxial bending and in-plane normal forces. The details and results of the test program are described, and the observed behavior patterns are discussed. The test data obtained are analyzed to corroborate constitutive models currently available for representing the effects of post-cracking tensile stresses in concrete. The ability of nonlinear finite element analysis procedures to accurately model shell element behavior is also examined.

Nonlinear finite element analyses are becoming more routine for use in examining critical details in the design of concrete shells.[1-3] In such cases, an accurate assessment of performance will depend on the finite element program's ability to model important second-order effects. Factors such as concrete compression softening, concrete tension stiffening, material nonlinearities, and geometric nonlinearities can exert a major influence on the predicted behavior of the structure.

In the response of shell elements subjected to primarily bending forces, the influence of post-cracking tensile stresses in the concrete (i.e., the tension-stiffening effect) is particularly important. Thus, the constitutive models used by the finite element program must accurately simulate these post-cracking concrete tensile stresses. Various formulations have been proposed in an attempt to do this.[4,5] Unfortunately, the majority of the formulations were developed using data obtained from tests on membrane elements subjected to in-plane forces. Experience has shown that they tend to overestimate the stiffening effect when applied in flexural-type problems. Few data exist from shell elements subjected to uniform biaxial flexural conditions combined with in-plane forces.

Thus, a limited-scope experimental investigation was undertaken involving the testing of large-scale shell elements. The objectives were to: 1) observe the phenomenological behavior of shell elements subjected to combined bending and membrane loading conditions; 2) provide data useful in spot-checking available tension-stiffening formu-
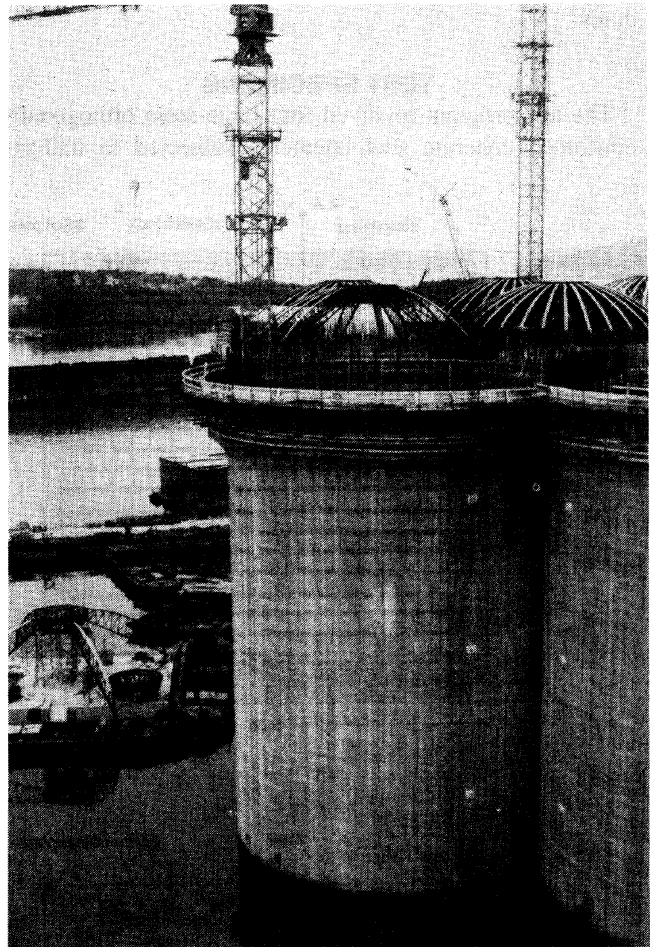

Fig. 1—Example of offshore concrete shell structure

Maria Anna Polak is an assistant professor of civil engineering at the University of Waterloo, Waterloo, Ontario, Canada. She received her MSc degree from the Technical University of Cracow, Poland, and her PhD degree from the University of Toronto. Her research activities include problems related to constitutive modeling and finite element analysis of reinforced concrete structures. She is a member of ACI Committee 435, Deflection of Concrete Building Structures; and joint ACI-ASCE Committee 445, Shear and Torsion.

Frank J. Vecchio is a profesor of civil engineering at the University of Toronto. His research interests include constitutive modeling and finite element analysis of reinforced concrete. He is a member of joint ACI-ASCE Committee 447, Finite Element Analysis of Reinforced Concrete Structures.

lations; and 3) provide corroboration of the accuracy of nonlinear finite element analysis procedures.

RESEARCH SIGNIFICANCE

This paper provides the details and results of tests conducted on shell elements under highly controlled and uniform loading conditions. Such data, currently sparsely available in the literature, will be valuable in corroborating theoretical material behavior models and analysis procedures.

TEST SPECIMENS

The test program involved four large-scale orthogonally reinforced concrete shell elements subjected to uniform loads. The panels were 1524 x 1524 mm (60 x 60 in.), with a thickness of 316 mm (12.4 in.). High-strength concrete was used in constructing the panels.

Fig. 2 provides a schematic diagram of the specimen configuration. Orthogonal in-plane reinforcement was placed in two layers. The in-plane reinforcement was welded to steel end-plates which, in turn, were attached to connector blocks. The connector blocks were mated to loading yokes, which attached to the actuators of the testing facility.

The tests were conducted using the shell element tester facility at the University of Toronto (see Fig. 3). Using two layers of in-plane actuators and a system of out-of-plane actuators to apply load along the edges of the test element, a wide range of loading combinations of bending moments, in-plane forces, and out-of-plane forces could be achieved. In this test series, only in-plane forces and bending moments were applied. The loading cases were such that forces were uniform throughout the test panel.

The test parameters included the loading condition and reinforcement orientation (see Fig. 4). The percentage of reinforcement provided was essentially the same for each specimen, with one direction being much more heavily reinforced than the other. In Panels SM1, SM2, and SM3, the reinforcement was placed parallel to the panel edges; in Panel SM4, the reinforcement was placed at 45 deg to the
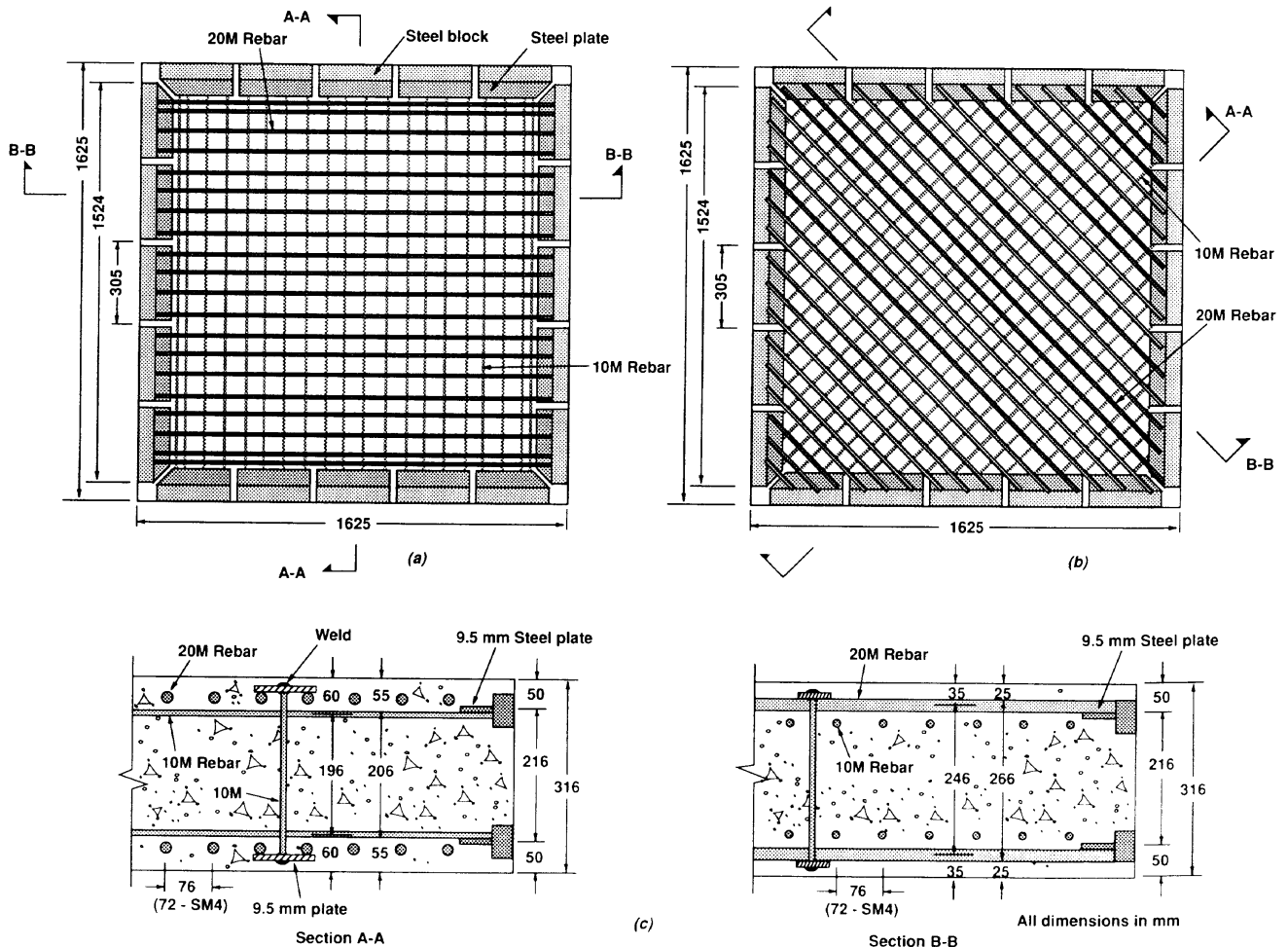

Fig. 2—Specimen details: (a) Specimens SM1 through SM3; (b) Specimen SM4; (c) cross-sectional details (1 mm = 0.0394 in.)

edges. Specimen SM1 was loaded in pure uniaxial bending along the stronger reinforcement direction. The loading of Specimen SM2 involved uniaxial bending coupled with biaxial in-plane forces, with tension applied in-line with the stronger reinforcement and compression applied along the weaker reinforcement. Specimen SM3 was tested in pure biaxial bending. Specimen SM4, with skew-directional reinforcement, was loaded in the same manner as SM2. The loads were applied in constant proportion, as given in Fig. 4.

The percentage of in-plane reinforcement provided in the strong direction (x-direction) was 1.25 percent per layer for Specimens SM1 through SM3, and 1.32 percent per layer for Panel SM4. In the weak direction (y-direction), the reinforcement ratio was 0.42 percent per layer for SM1 through SM3, and 0.44 percent for SM4. No. 20M bars at approximately 75-mm (3-in.) centers were used for the x-direction reinforcement, and No. 10M bars at approximately 75-mm (3-in.) centers were used for the y-direction reinforcement. In all specimens, a small amount (0.07 percent) of out-of-plane reinforcement was provided in the form of T-headed No. 10M bars.

The panels were cast using concrete obtained from a local ready-mix supplier. A compressive strength of 35 MPa (5.1 ksi) was specified, along with a maximum aggregate size of 10 mm (0.4 in.) and a 50-mm (2-in.) slump. The material properties of the concrete obtained were determined from 300 x 150-mm (12 x 6-in.) cylinders tested at approximately the same time as the panels. The properties are summarized in Table 1(a), and representative compression stress-strain curves are given in Fig. 5(a). Note that the compressive strengths obtained were substantially higher than specified.

The No. 20M bars used for the x-direction reinforcement were found to exhibit a well-defined yield plateau. Conversely, the No. 10 M bars initially did not, and were therefore subjected to heat- treating. After heat-treating, the stress-strain behavior of the No. 10 M bars was essentially trilinear in nature. The material properties of the reinforcey trilinear in nature. The material properties of the reinforcement, obtained from coupon tests, are summarized in Table
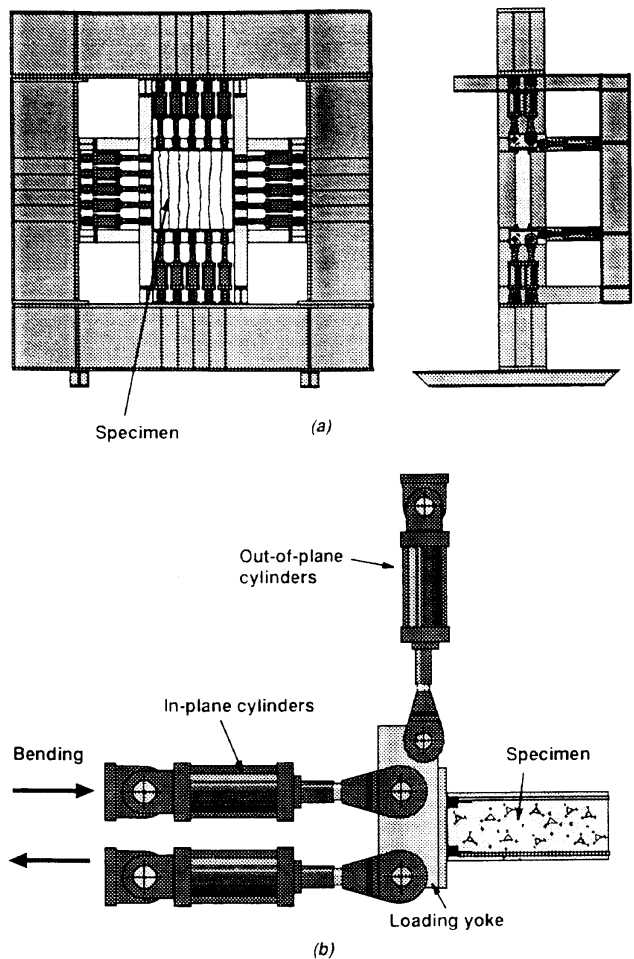

Fig. 3—Shell element tester facility: (a) schematic view of tester; (b) specimen connection details

1(b). Typical stress-strain response curves are shown in Fig. 5(b).

Instrumentation of the test panels included linear variable displacement transducers (LVDTs), mechanical strain gage targets on the panel surfaces, and electrical strain gages

Name	Concrete f_c' (MPa)	Reinforcement Pattern	X - Reinforcement		Y - Reinforcement		Loading Pattern	Loading Ratio
			ρ_x* (%)	f_{yx} (MPa)	ρ_y* (%)	f_{yy} (MPa)		
SM1	47		1.25	425	0.42	430		
SM2	62		1.25	425	0.42	430		$\frac{M}{P} = 0.25$ m
SM3	56		1.25	425	0.42	430		$\frac{M_1}{M_2} = 3.2$
SM4	64		1.32	425	0.44	430		$\frac{M}{P} = 0.25$ m

* Per layer

Fig. 4—Test parameters (1 MPa = 0.145 ksi, 1 m = 39.4 in.)

Table 1(a)— Material properties of concrete

Specimen	Compressive peak strength, f_c' MPa	Strain at peak stress, ε_0 $\times 10^{-3}$	Tensile strength f_{ct} MPa	Age at testing t, days
SM1	47	2.00	2.78	60
SM2	62	2.60	3.16	150
SM3	56	2.65	2.6	120
SM4	64	2.60	2.76	150

Table 1(b)— Material properties of reinforcement

| Type	Diameter D, mm	Area A_S, mm^2	Yield Stress f_y, MPa	Harden strain ε_h, $\times 10^{-3}$	Ultimate stress f_u, MPa	Ultimate strain ε_u, $\times 10^{-3}$
20M	19.5	300	425	25.0	611	150.0
10M	11.3	100	430	40.0	480	75.0

1 mm = 0.039 in.; 1 MPa = 0.45 ksi.

applied to the reinforcement. The LVDTs provided a measure of the panel deformations during testing, and were used only to assist in conducting the test. The measurements of strain used to analyze panel behavior were those obtained from the mechanical strain gages equipped with electronic feedouts, monitored by a computer- controlled data acquisition system. Target points were placed on a 7 x 7 grid, with a 200-mm (8-in.) grid spacing on each surface of the test panel. Readings were taken in the *x*- and *y*-directions and in the two diagonal directions, for a total of 156 strain readings on each side. Electrical resistance strain gages of 10-mm (0.4-in.) length were used to monitor the strains in the in-plane and out-of-plane reinforcement. The loads acting on the panels were calculated from hydraulic pressure measurements, using calibration factors previously determined for each actuator. Several load cells were also used to confirm the applied load conditions.

Loads were applied to the test panels in a monotonically increasing manner. At discrete stages in the loading, loading was suspended and deformations were held constant while the mechanical strain gage readings were taken. Testing of each specimen required about 2 to 3 days. The specimens were unloaded at the end of each day. A view of a panel during testing is shown in Fig. 6.
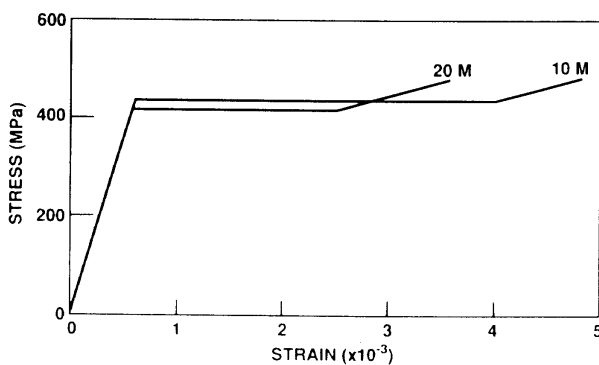
SPECIMEN BEHAVIOR

A summary and comparison of the loading history of the test panels is given in Table 2 and in Fig. 7.
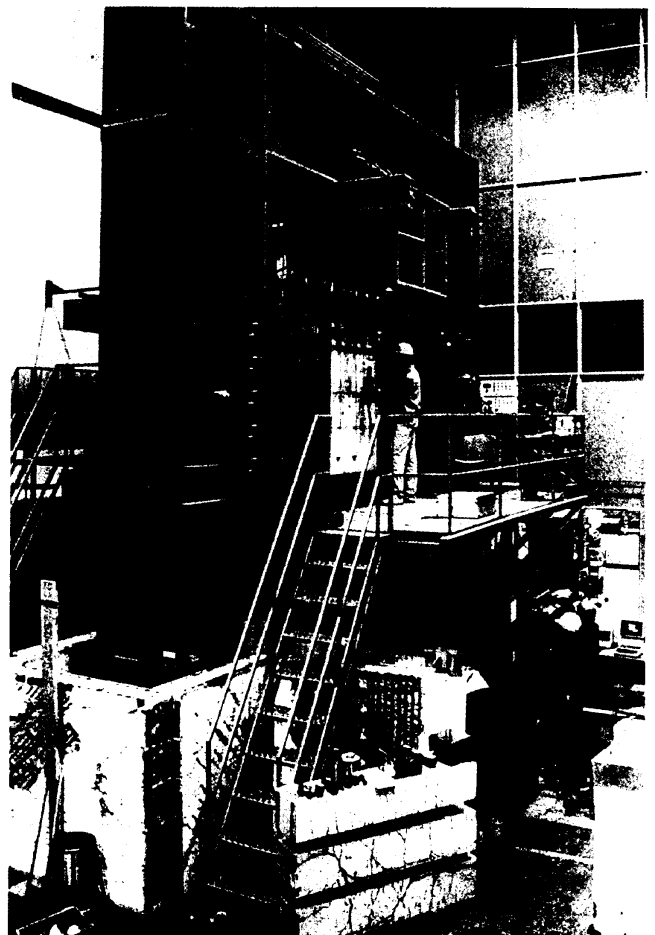
Specimen SM1 was subjected to pure uniaxial bending

Fig. 5—Typical stress-strain curves: (a) concrete; (b) reinforcement (1 MPa = 0.145 ksi)
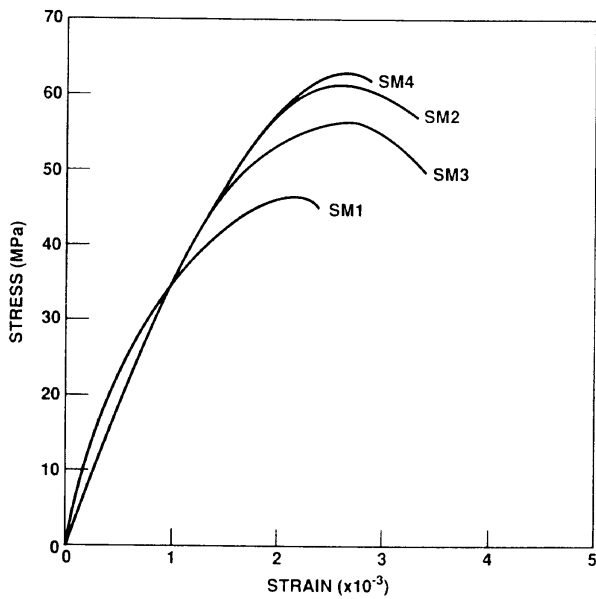
Fig. 6—Specimen during testing

along the stronger reinforcement direction. The panel cracked at a moment of 75 kN·m/m (16.9 kip-ft/ft), with a sudden drop in stiffness. A uniform crack pattern developed with a crack spacing of approximately 100 mm (4 in.). The load-deformation response between the cracking and yielding stages was almost linear in nature. First, yielding occurred at a moment of 440 kN·m/m (98.9 kip-ft/ft), accompanied by an average crack width of 0.3 mm (0.012 in.). Beyond yielding, the flexural stiffness was much reduced, but the panel continued to carry increased load. Loading was terminated at an ultimate moment of 464 kN·m/m (104.3 kip-ft/ft) due to excessively large deformations.

Specimen SM2, similar in construction to SM1, was subjected to biaxial in-plane forces in addition to the uniaxial bending. The influence of the in-plane tension was, as expected, to reduce the cracking [45 kN·m/m (10.1 kip-ft/ft)], yielding [302 kN·m/m (67.9 kip-ft/ft)], and ultimate [421 kN·m/m (94.6 kip-ft/ft)] moments. The stiffness of the load-deformation response was also reduced at all stages. Again, the cracks were uniformly spaced at approximately 100 mm (4 in.), and the average crack width at yielding was 0.3 mm (0.012 in.). As with panel SM1, the test was terminated because of excessively large deformations without any apparent signs of concrete crushing.

Specimen SM3, also similar in construction to SM1, was subjected to pure biaxial bending. Compared to the behavior of SM1, the presence of the transverse bending is seen to have little influence on the response in the strong direction. The cracking moment [62 kN·m/m (13.9 kip-ft/ft)] was reduced by about 20 percent, despite the stronger concrete. The yield moment [435 kN·m/m (97.8 kip-ft/ft)] and the ultimate moment [488 kN·m/m (109.7 kip-ft/ft)], however, were essentially the same as observed with SM1. Yielding in the x- and y-directions occurred at approximately the same stage of loading. At yielding, the crack spacing was about 100 mm (4 in.) for cracks parallel to the 10M bars, and about 200 mm (8 in.) for cracks parallel to the 20M bars. The average crack width in each direction was 0.3 mm (0.012 in.). At ultimate load, concrete on the compression face of the panel crushed in a direction normal to the higher applied moment.

Specimen SM4 had essentially the same reinforcement percentages and imposed loading as Panel SM2, but with the reinforcement oriented at 45 deg to the loading directions. Compared to SM2, the observed behavior was significantly different. The cracking moment [51 kN·m/m (11.5 kip-ft/ft)] was unaffected. The yield moment [160 kN·m/m (36 kip-ft/ft)] and the ultimate moment [205 kN·m/m (46 kip-ft/ft)], however, were approximately half of those observed in SM2. Further, the nature of the load-deformation response was appreciably altered. After cracking, the panel's response was highly nonlinear, with no definite point of yielding discernible. Initial cracking occurred normal to the applied tensile load. As load was increased and yielding of the y-reinforcement was approached, the direction of the cracks rotated toward the direction of the stronger reinforcement. At yielding, the cracks had an average spacing of 50 mm (2 in.) and an average width of 0.7 mm (0.030 in.), and were inclined at about 10 deg to the x-direction. The test
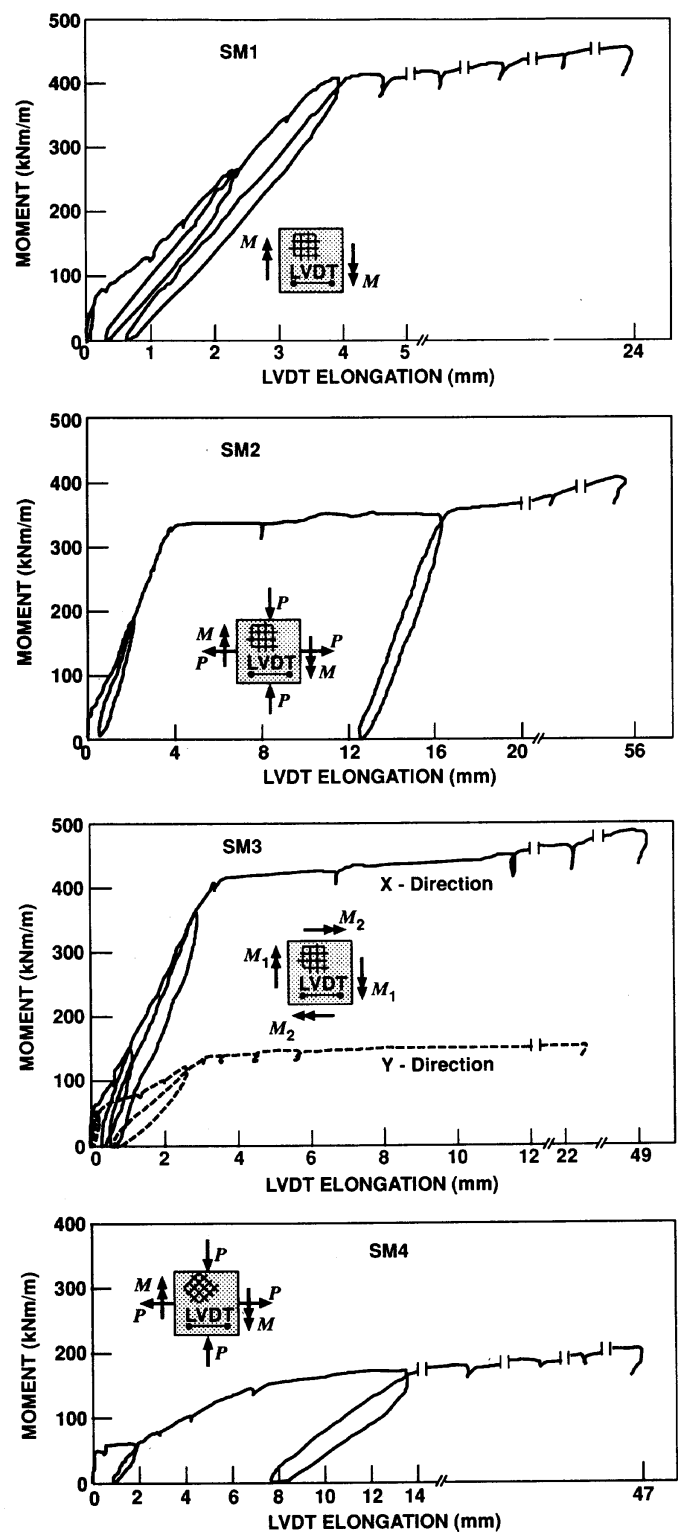

Fig. 7—Observed load-deformation response of test specimens: (a) SM1; (b) SM2; (c) SM3; (d) SM4 (1 mm = 0.0394 in.; 1kN·m/m = 0.225 kip-ft/ft)

was terminated when, at very large deformation levels, a single large crack opened up.

In general, the load-deformation response of each specimen was essentially trilinear. The general tendency was that, just after cracking, the stiffness of the panels would drop significantly. However, after the tensile surface strains reached a magnitude slightly greater than the theoretical

Table 2— Summary and comparison of loading history of test panels

Specimen	Observed response, kN•m/m			Predicted response, kN•m/m			Observed/predicted ratio		
	M_{cr}	M_y	M_u	M_{cr}	M_y	M_u	M_{cr}	M_y	M_u
SM1	75	437	477	85	450	475	0.88	0.97	1.00
SM2	45	302	421	85	290	320	0.90	1.04	1.32
SM3-X	62	435	488	75	440	470	0.83	0.99	1.04
SM3-Y	55	138	151	75	140	145	0.74	0.99	1.04
SM4	51	160	205	55	155	170	0.93	1.03	1.20

1 kN.m/m = 0.225 kip-ft/ft.

cracking strain, the element stiffness would again increase. Specimens SM1, SM2, and SM3 were loaded in directions parallel to the reinforcement. Yielding in these panels was well defined, with a sudden and almost complete loss in stiffness. Conversely, the behavior of Panel SM4 was governed first by yielding of the weaker reinforcement and finally by yielding of both reinforcements. The decay in stiffness of SM4 was much more gradual. Just prior to yielding, the cracks in SM4 had rotated about 8 deg from the direction of the applied tension force. After yielding of the y-reinforcement, the crack rotation became much more prominent. The tension face of Specimen SM4, at failure, is shown in Fig. 8. In all cases, the panels were able to achieve deformations several times greater than the yield levels.

ANALYSIS OF TEST DATA

The test results were analyzed to determine the nature of the effective tensile forces in the concrete arising from tension- stiffening mechanisms. From the experimental values of the concrete and reinforcement strains, and using appropriate constitutive relations, the reinforcement stresses and concrete compressive stresses were found. Knowing these
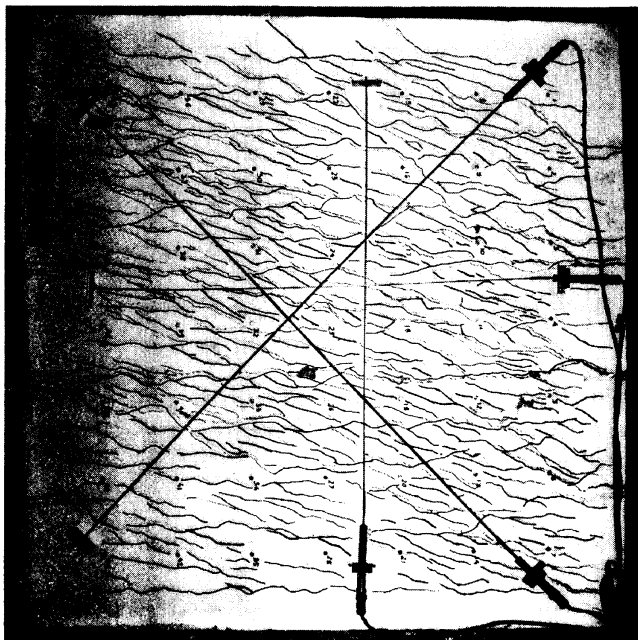

Fig. 8—Specimen SM4 at ultimate load

stresses, and given the applied loading on the section, the magnitude and location of the effective concrete force required to maintain equilibrium was determined.

The constitutive law used for modeling the compressive behavior of concrete was that proposed by Vecchio and Collins.[4] Poisson's ratio was assumed to be 0.15 for uncracked concrete, and zero for cracked concrete. Calculation of concrete stresses was done using a layered model.

Shown in Fig. 9 are the representative results obtained for Element SM1. They confirm the existence of significant levels of tensile stress in the cracked concrete of elements subjected to bending. Shown also are the concrete tensile forces predicted using the tension-stiffening model proposed by Izumo et al.[5] Good agreement was obtained, although the theoretical stresses tended to be generally higher than those observed. The results for the other elements were somewhat more scattered and inconclusive.

FINITE ELEMENT MODELING

The behavior of the test specimens was modeled using the nonlinear finite element program APECS.[*] The program is a secant stiffness-based procedure embodying the assumptions of the modified compression field theory,[4] using a smeared, rotating crack modeling approach. The degenerate isoparametric shell elements available are specially formulated to allow for the influence of out-of-plane shear deformations and other second-order effects. The influence of changing structural geometry is considered through the
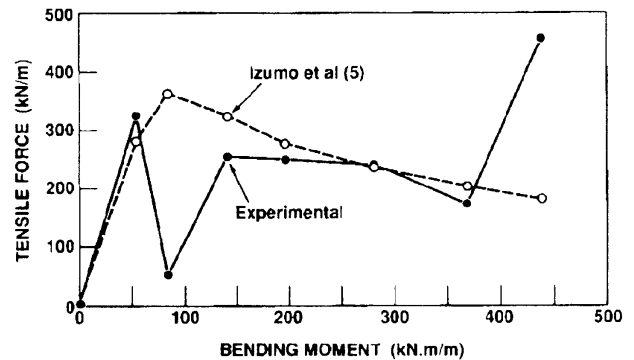
Fig. 9—Correlation of test data to theoretical tension-stiffening formulation (1 kN/m = 0.0685 kip/ft, 1 kN•m/m = 0.225 kip-ft/ft)
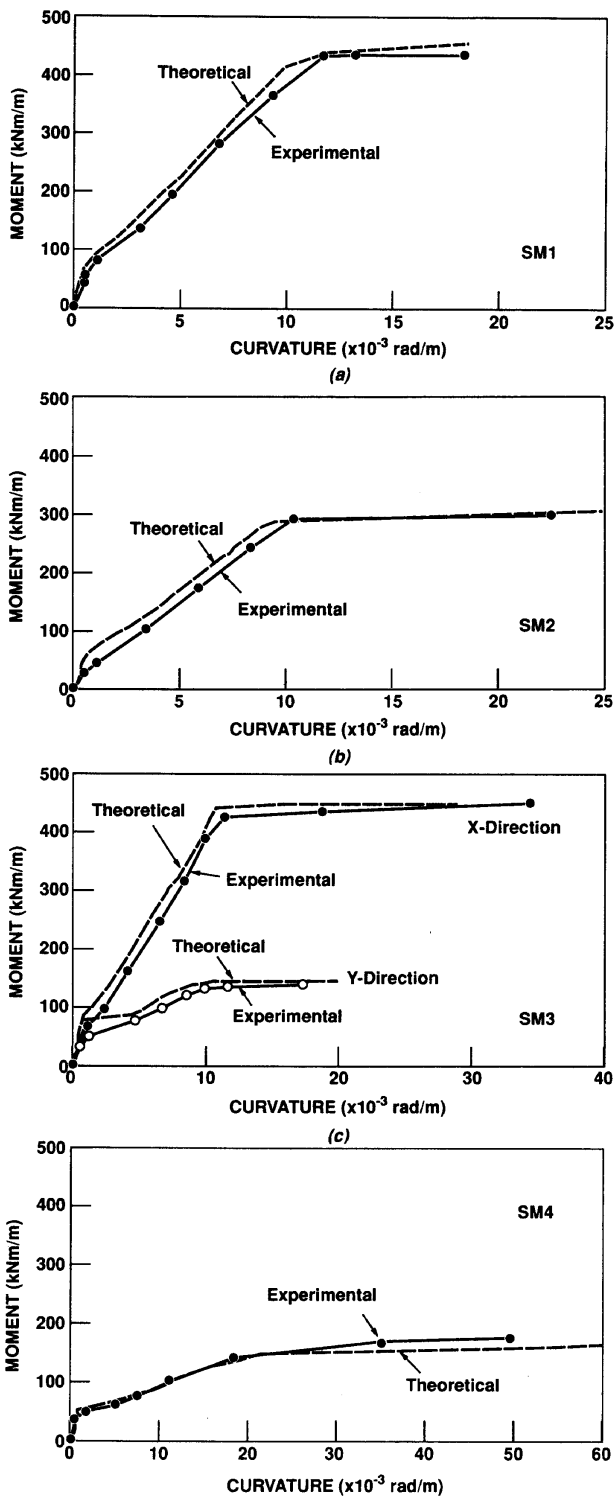
Fig. 10—Comparison of experimental and theoretical moment-curvature response: (a) SM1; (b) SM2; (c) SM3 in x-direction; (d) SM3 in y-direction (1 kN•m/m = 0.225 kip-ft/ft)
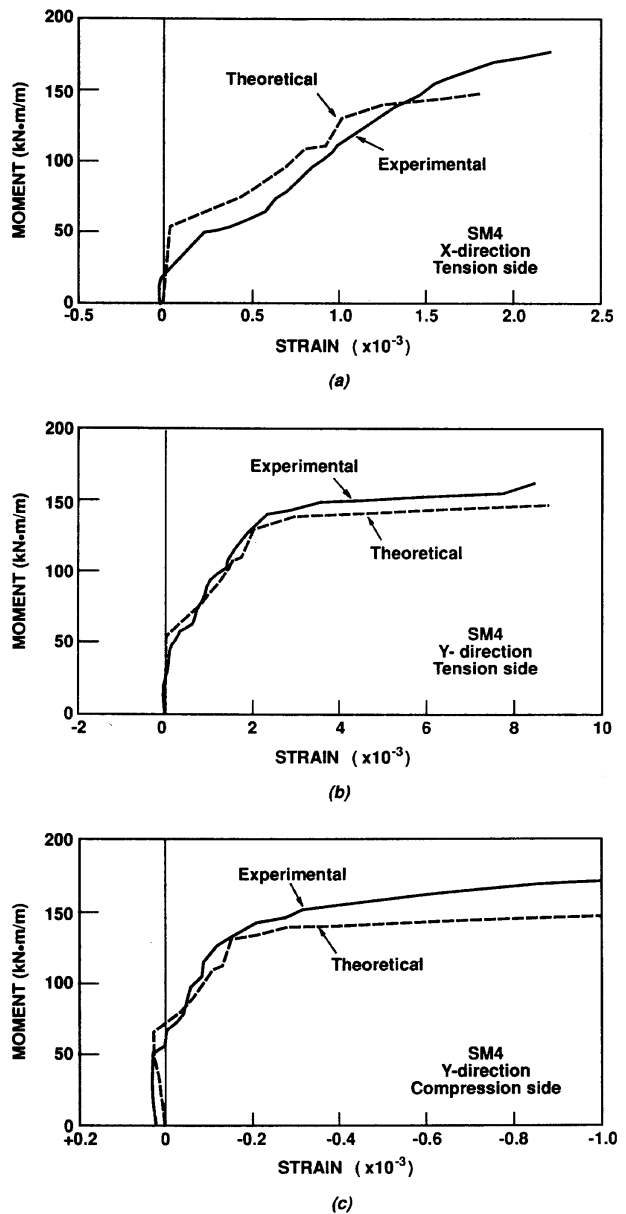

Fig. 11—Comparison of experimental and theoretical reinforcement strains for SM4: (a) x-direction, tension side; (b) y-direction, tension side; (c) y-direction, compression side (1 kN•m/m = 0.225 kip-ft/ft)

implementation of a total Lagrangian formulation. Material nonlinearities are accounted for by the use of appropriate constitutive relations. In this application, the tension- stiffening model used was that suggested by Izumo et al.[5] For the reinforcement, an elastic-plastic response curve was used.

The test specimens were modeled using nine equal-size elements. The element used was a nine-noded 42-degree-of-

freedom heterosis element with selective integration.* Both the in-plane and out-of-plane reinforcement were modeled in a smeared manner. The material properties used in the analyses were those reported in Table 1.

Compared in Table 2 are the predicted and observed moments at cracking, yielding, and ultimate. Generally, the cracking moments of the panels were overestimated, with a mean experimental-to- predicted value of 0.85. The large thickness of the elements, possibly leading to shrinkage stresses, may have been partially responsible. The correlation

of the yield moments was very good, with a mean experimental-to-theoretical value of 1.00 and a coefficient of variation of 3.0 percent. The ultimate moment capacities were somewhat underestimated (mean of 1.11). However, the tests were taken to extremely large deformation levels. Influences from strain hardening and from testing facility interference may have affected results.

More representative comparisons of the theoretical and experimental responses are made in the moment-curvature behaviors shown in Fig. 10. Very good correlation is seen in all phases of response, including precracking stiffness, post-cracking stiffness, and post-yielding behavior. Similarly, good correlation was obtained in modeling tensile surface strains and compressive surface strains. Crack rotations in SM4 were also modeled well.

Shown in Fig. 11 are comparisons of the theoretical and experimental reinforcement strains in Panel SM4. This specimen was most affected by tension-stiffening effects and crack modeling assumptions, owing to the rotation of cracks and redistribution of forces that occurred. Again, very good correlation was achieved.

CONCLUSIONS

Tests were conducted on four large-scale reinforced concrete shell elements. Loading conditions involved biaxial bending combined with in-plane forces.

It was observed that when the imposed loads were in line with the reinforcement, there was little interaction between the orthogonal directions except for a possible lowering of the cracking moments. On the contrary, when the loads were skew to the reinforcement, response was appreciably more nonlinear, with redistribution of forces and reorientation of cracks apparent. In-plane forces were also seen to significantly affect flexural response.

The tension-stiffening models developed for membrane elements were found to somewhat overestimate the effect in flexural elements. Nevertheless, they were useful in modeling behavior to an acceptable degree of accuracy. Further experimental and theoretical work is required in this area.

The nonlinear finite element analysis procedures used were found to model accurately the response of the test specimens. Precracking, post-cracking, and post-yielding behavior were all simulated well. Essential to the good correlations obtained was the use of a constitutive model representing post-cracking tensile stresses in the concrete.

NOTATION

A_s = cross-sectional area of reinforcing bar

D = diameter of reinforcing bar

E_s = modulus of elasticity of reinforcing steel

f_c' = compressive strength of concrete (cylinder)

f_{ct} = tensile strength of concrete

f_u = ultimate stress of reinforcing steel

f_y = yield stress of reinforcing steel

M_{cr} = cracking moment

M_y = yield moment

M_u = ultimate moment

ε_0 = strain at peak cylinder stress

ε_h = strain at commencement of strain hardening

ε_u = ultimate strain of reinforcement

ρ_x = reinforcement ratio in x-direction

ρ_y = reinforcement ratio in y-direction

REFERENCES

1. Scordelis, A. C., and Chan, E. C.,"Nonlinear Analysis of Reinforced Concrete Shells," *Computer Applications in Concrete Technology,* SP-98, American Concrete Institute, Detroit, 1987, pp. 25-57.

2. Balakrishnan, S., and Murray, D. W.,"Concrete Constitutive Model for NLFE Analysis of Structures," *ASCE Journal of Structural Engineering,* V. 114, No. 7, July 1988, pp. 1449-1466.

3. Massicotte, B.; MacGregor, J. G.; and Elwi, A. E.,"Behaviour of Concrete Panels Subjected to Axial and Lateral Loads," *ASCE Journal of Structural Engineering,* V. XX, No. X, Sept. 1990, pp. 2324-2343.

4. Vecchio, F. J., and Collins, M. P.,""Modified Compression Field Theory for Reinforced Concrete Elements Subjected to Shear," ACI JOURNAL, *Proceedings* V. 83, No. 2, Mar.-Apr. 1986, pp. 219-231."

5. Izumo, J.; Shin, J.; Maekawa, K.; and Okamura, H.,"Analytical Model for RC Panels Subjected to In-Plane Stresses," *Concrete Shear in Earthquake,* Elsevier Applied Science, New York, 1992, pp. 206-215.